Available online at www.sciencedirect.com
SCIENCE DIRECT®
Marine Micropaleontology 48 (2003) 49–70
MARINE MICROPALEONTOLOGY
www.elsevier.com/locate/marmicro

Western Mediterranean planktonic foraminifera events and millennial climatic variability during the last 70 kyr

M. Pérez-Folgado [a,*], F.J. Sierro [a], J.A. Flores [a], I. Cacho [b], J.O. Grimalt [c], R. Zahn [d], N. Shackleton [b]

[a] *Department of Geology, University of Salamanca, Plaza de la Merced, 37008 Salamanca, Spain*
[b] *University of Cambridge, The Goldwin Laboratory, Pembroke Street, Cambridge CB2 3SA, UK*
[c] *Department of Environmental Chemistry, Institute of Chemical and Environmental Research (CSIC), Jordi Girona, 18, 08034 Barcelona, Spain*
[d] *G.R.C. Marine Geosciences, Department of Stratigraphy and Paleontology, University of Barcelona, 08071 Barcelona, Spain*

Received 12 June 2002; received in revised form 14 October 2002; accepted 16 October 2002

Abstract

Detailed study of associations of planktonic foraminifera in cores MD95-2043 and ODP 977, located in the Alboran Sea (Mediterranean Sea), has allowed the identification of 29 new faunal events, defined by abrupt changes in the abundances of *Neogloboquadrina pachyderma* (right and left coiling), *Turborotalita quinqueloba*, *Globorotalia scitula*, *Globorotalia inflata*, *Globigerina bulloides* and *Globigerinoides ruber* (white and pink varieties). The age model for ODP 977 was based on that of MD95-2043 [Cacho et al. (1999), Paleoceanogr. 14, 698–705], on the isotopic stratigraphy, and on two AMS ^{14}C measurements. Sea Surface Temperatures (SSTs) were estimated for the last 54 kyr using the Modern Analog Technique (MAT) and were compared with the SSTs provided by the $U^{k'}_{37}$ method. The $U^{k'}_{37}$ record is very similar to the MAT annual mean temperature record for the last 8 kyr. However, for older times alkenone-derived temperatures are consistently higher than the annual MAT temperatures. This offset may be due to an underestimation of the SST provided by the planktonic foraminiferal method for glacial times, to an overestimation of the $U^{k'}_{37}$ record, or to changes in the seasonal production of alkenones. Most of the variability in the fauna is related to the millennial variability of Heinrich and Dansgaard–Oeschger (D–O) events. During Heinrich events (HEs) and most of the other D–O stadials, *G. bulloides*, *T. quinqueloba* and *G. scitula* increased, while *N. pachyderma* (right coiling), *G. inflata* and *G. ruber* decreased. By contrast, *N. pachyderma* (left coiling) was only abundant in the HEs. The main component of the associations – *N. pachyderma* (right coiling) – follows a general trend similar to that of sea-level and δ^{18}O. This species reached its highest abundance during the Last Glacial Maximum, when sea-level was at a lower position. The occurrence of a shallower nutricline owing to a shallowing of the interface between Atlantic inflowing and Mediterranean outflowing waters could have favoured the development of neogloboquadrinids in the vicinity of the Strait of Gibraltar.

Keywords: Late Quaternary; millennial variability; planktonic foraminifera biostratigraphy; western Mediterranean; palaeotemperatures; palaeoceanography

* Corresponding author. Tel.: +34-923-294497; Fax: +34-923-294514.
E-mail address: martap@usal.es (M. Pérez-Folgado).

0377-8398/02/$ – see front matter © 2002 Elsevier Science B.V. All rights reserved.
PII: S0377-8398(02)00160-3

1. Introduction

The Mediterranean Sea is a semi-enclosed marginal basin connected with the Atlantic through the Strait of Gibraltar, a threshold with a depth of 284 m (Bryden and Kinder, 1991). Its negative water balance (precipitation+evaporation < 0; Bethoux, 1979) results in an anti-estuarine circulation responsible for the oligotrophic Mediterranean conditions. Likewise, because it is a closed basin located in a temperate climatic belt, all climatic events are usually amplified with respect to the surrounding basins.

In the Alboran Sea, the Modified Atlantic Water (MAW) flows into the Mediterranean at the surface (Fig. 1), while the Mediterranean Outflowing Water (MOW) flows out of the Mediterranean at depth. The MAW forms an almost homohaline band (36.5‰), extending to 150–200 m depth, which in winter is almost homothermal (15°C) (Fig. 2; Parrilla and Kinder, 1987; Tintoré et al., 1988). This water mass describes two anticyclonic gyres – western and eastern (Fig. 1) – which are the most characteristic features of the surficial circulation in the Alboran Sea, especially the western gyre (Parrilla, 1984; Heburn and La Violette, 1990). Below the MAW, the Levantine Intermediate Water (LIW), down to an approximate depth of 600 m (Fig. 2), and the deep water formed in the Gulf of Lyon (Western Mediterranean Deep Water, WMDW) are the main components of the MOW, which flows out of the Mediterranean through the Strait of Gibraltar. These two water masses (LIW and WMDW) have high salinities (about 38.5%) although the WMDW is slightly colder (12.90°C) than the LIW (13.2°C), as may be seen in Fig. 2 (Parrilla and Kinder, 1987).

The Alboran Sea is one of the most productive regions in the Mediterranean due to the interaction between inflowing MAW and outflowing intermediate Mediterranean water. The position of the anticyclonic gyres governs the water depth of the pycnocline, located at the site of interference between MAW and MOW. This pycnocline is deeper towards the central part of the gyres, while isopicnals rise in the cyclonic structures that appear at the North side of the basin, particularly in the upwelling off the coast of Málaga, favouring the nutrient supply to surface waters (Rodríguez et al., 1998). The upwelled nutrients in the north are then advected towards the south, following the paths of the main gyres (García-Gorriz and Carr, 2001). Nutrients are also supplied to the

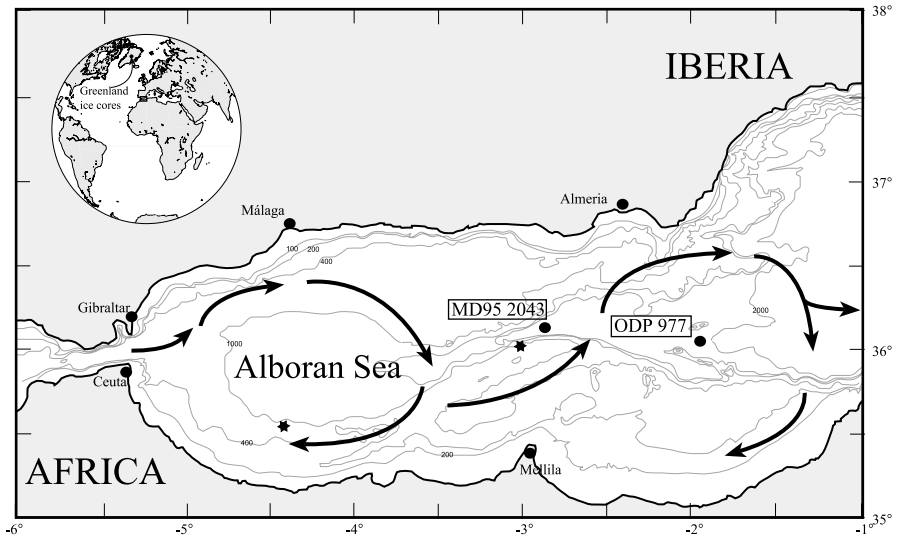

Fig. 1. Location of cores ODP 977 and MD95-2043 in the Alboran Sea. The figure shows the main features of the current circulation, governed by the entry of surface waters through the Strait of Gibraltar, and the formation of anticyclonic gyres (Heburn and La Violette, 1990). Black asterisks mark the location of points in Fig. 2.

surface by eddy-induced upwelling occurring at the periphery of the gyre path (García-Gorriz and Carr, 2001). Based on the temporal distribution of pigment concentrations in the Alboran Sea, two main regimes of primary production have been distinguished (García-Gorriz and Carr, 2001): the *bloom* regime (from November to March), linked to the winter destratification, and the *non-bloom* period (from May to September), when surface water stratification prevails in the Alboran Sea and nutrients are mainly advected from the different upwelling zones.

In the past few years, several biostratigraphic works have been published concerning the Pleistocene–Holocene of the Mediterranean (Pujol and Vergnaud-Grazzini, 1989; Capotondi et al., 1999). Recently, however, climatic and palaeoceanographic studies undertaken within the IMAGES programme have aimed at monitoring the climatic variations at millennial scale, meaning that it has been necessary to develop more precise age models that will allow researchers to obtain reliable correlations.

The aims of the present work are to define a biostratigraphy and process-oriented faunal interpretation at millennial scale, in a region that is very sensitive to the exchange transports in the Strait of Gibraltar, and also to assess the applicability of the stratigraphic framework to general western Mediterranean faunal studies. Based on a well-established age model (by use of oxygen isotope stratigraphy and ^{14}C-dated ages) and a high resolution study of the planktonic foraminifera fauna in two cores from the Alboran Sea (ODP 977 and MD95 2043), we attempt to define a series of bio-events, most of them common to both cores. The identification of these bio-events in other more or less distant cores could permit a precise correlation among them and facilitate palaeoclimatic and/or palaeoceanographic interpretations for the last 70 kyr.

2. Materials and methods

MD95-2043 is a piston core, of which the first 17 m were studied. It was recovered from the eastern part of the Alboran Sea (36°8′598″N, 2°37′269″W; 1841 m water depth) by the R/V *Marion Dufresne* during the 1995 IMAGES cruise (Fig. 1). ODP 977 was recovered during leg 161 of the Ocean Drilling Program carried out in the western Mediterranean. It is located to the south of Cabo de Gata (Spain), also in the eastern Alboran Basin (36°1.9′N, 1°57.3′W; 1984 m water depth). For this core, the first 27 m were studied, although here we only offer results for the first 13 m.

In both cores, systematic samplings were made for the study of the microfauna at an average distance of 10 cm. The samples for the analysis of planktonic foraminifera were washed through a 62-μm sieve and dry-sieved again through a 150-μm mesh. The residues (>150 μm) were split the number of times necessary to obtain an aliquot fraction of some 350 specimens, which were counted and identified (Appendix Tables 1 and 2 as **Marine Micropaleontology Online Background Dataset**[1]). To calculate the abundance of *Neogloboquadrina pachyderma* left coiling (l.c.), an aliquot of around 1000 specimens was analysed (Appendix Table 1[1]). Oxygen and carbon isotope measurements were performed on the planktonic foraminifer *Globigerina bulloides* and on the benthic foraminifer *Cibicidoides* spp. In core MD95-2043, analyses were made on a SIRA mass spectrometer on the 300–355-μm fraction (Cacho et al., 1999[1]), while samples from ODP 977 were measured on a Finnigan MAT 251 Device at the University of Kiel, the size of the fraction being 250–355 μm (Appendix Table 3[1]).

Seasonal palaeotemperatures in MD95-2043 were obtained using the Modern Analog Method (MAT; Hutson, 1980; Prell, 1985). This method uses a statistic distance (in our case, the 'squared chord distance'; Overpeck et al., 1985) called the 'dissimilarity index', which gives the relationship between fossil and current assemblages. The final palaeo-SST is the weighted mean of the ten best analogs. The database used here was that of Kallel et al. (1997) for the Mediterranean Sea, which comprises 253 coretop samples (130 from the Mediterranean Sea, and 123 from the North

[1] http://www.elsevier.com/locate/marmicro

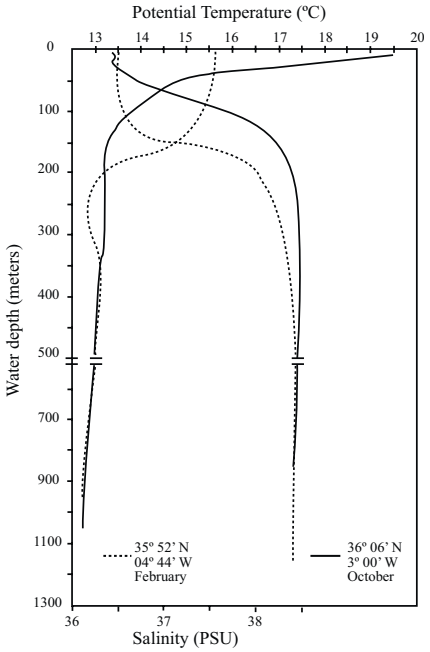

Fig. 2. Distribution of surface temperatures and salinity with depth at two points in the Alboran Sea during two different seasons of the year. The first 150–200 m of water correspond to Modified Atlantic Water; down to a depth of approximately 600 m is the Levantine Intermediate Water. The rest – down to the sea floor – corresponds to Western Mediterranean Deep Water. After Parrilla and Kinder, 1987. The locations are marked in Fig. 1 by black asterisks.

Atlantic Ocean). The average 'dissimilarity' obtained was 0.13 (varying between 0 and 0.4), and the mean error for all the reconstructions was ±1.85°C.

Finally, to check the relationship between the different species of planktonic foraminifera, we performed a Principal Component Analysis (PCA) on samples from ODP 977.

3. Age model

The age model for core MD95-2043 was established by Cacho et al. (1999) and is based on 21 AMS ^{14}C measurements and on isotopic stratigraphy. The age model for ODP 977 is based on two AMS ^{14}C measurements corresponding to the uppermost Holocene, the oxygen isotope results, and the accurate correlation of some planktonic foraminiferal events between this core and core MD95-2043 (see Table 1). The AMS ^{14}C analyses were performed on the planktonic foraminifer *Globigerina bulloides* and were calibrated to calendar years (Stuiver et al., 1998), using the Calib 4.1 programme. The oxygen isotope curves of both cores (Fig. 3) allowed us to identify the Last Glaciation (Marine Isotope Stage 2, MIS 2), together with isotope events 3.1 and 3.13 (Cacho et al., 1999; Martinson et al., 1987).

The sharp cold climatic events associated with massive discharges of icebergs, known as Heinrich Events (HEs), have been identified throughout the North Atlantic (Heinrich, 1988; Bond et al., 1992; Grousset et al., 1993; Lebreiro et al., 1996; Cayre et al., 1999). Ice Rafted Debris (IRD) accompanying the melting of the icebergs has been recognised as far as the Portuguese margin (Zahn et al., 1997), the Gulf of Cádiz, (Cacho et al., 2001; Reguera, 2001; Colmenero, 2001), and the Moroccan continental margin (Kudrass and Thiede, 1970; Kudrass, 1973).

To date no IRD record has been identified in the Mediterranean. However, *Neogloboquadrina pachyderma* (l.c.) proliferated in the Alboran Sea when conditions became favourable, especially when sea surface temperatures lowered during the HEs. Cacho et al. (1999) identified and dated

Table 1
Age model pointers for ODP 977

Depth ODP 977 (m)	Event	Age (calendar years)	Reference
0.202	AMS ^{14}C	1159	Stuiver et al., 1998
0.605	AMS ^{14}C	4220	Stuiver et al., 1998
2.952	HE1	15207	Cacho et al., 1999
4.150	HE2	23403	Cacho et al., 1999
5.212	HE3	30122	Cacho et al., 1999
7.615	HE4	38845	Cacho et al., 1999
9.553	HE5	45031	Cacho et al., 1999
12.404	HE6	65987	(*)

HE pointers are defined in event terminations in *Neogloboquadrina pachyderma* (l.c) curve, except for HE6, where the maximum abundance point in *N. pachyderma* (l.c.) percentage has been used. (*) Bond et al., 1992, 1993; Grousset et al., 1993; Lebreiro et al., 1996; Manighetti et al., 1995; Paterne et al., 1999; Chapman and Shackleton, 1998; van Kreveld et al., 1996; Cayre et al., 1999.

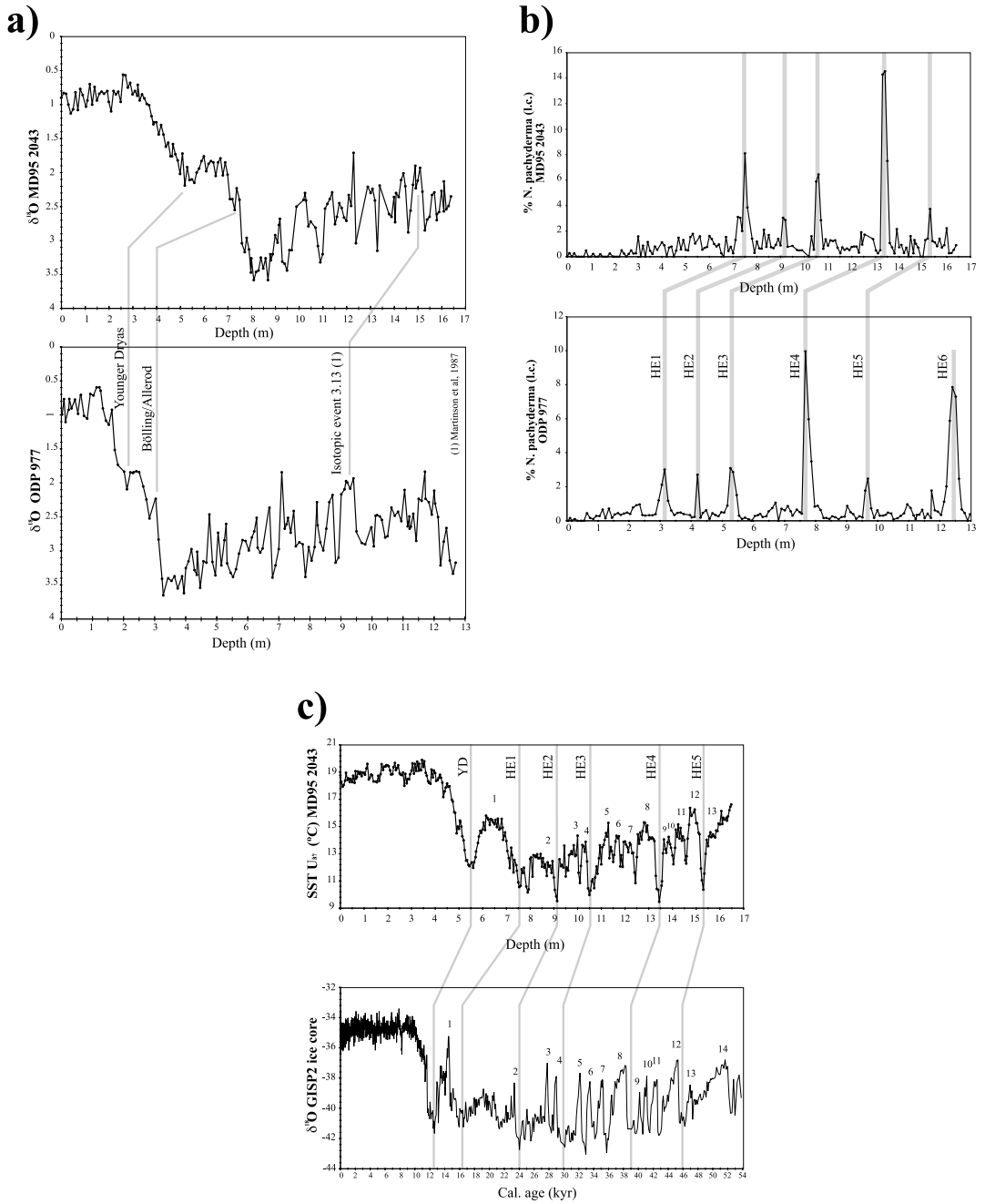

Fig. 3. Age model for core ODP 977. (a) Comparison of the isotopic results ($\delta^{18}O$) from core MD95-2043 (Cacho et al., 1999) with those for core ODP 977, highlighting the events used for the correlation. (b) Correlation between the curves of relative abundance of *Neogloboquadrina pachyderma* (l.c.) in both cores. The peaks in abundance have been correlated with HE1–HE6. (c) Correlation between the $\delta^{18}O$ curve in Greenland Ice Core GISP2 and the temperature curve obtained using the alkenone technique in MD95-2043 (Cacho et al., 1999). Numbers mark the different D–O interstadials, recognisable in both cores.

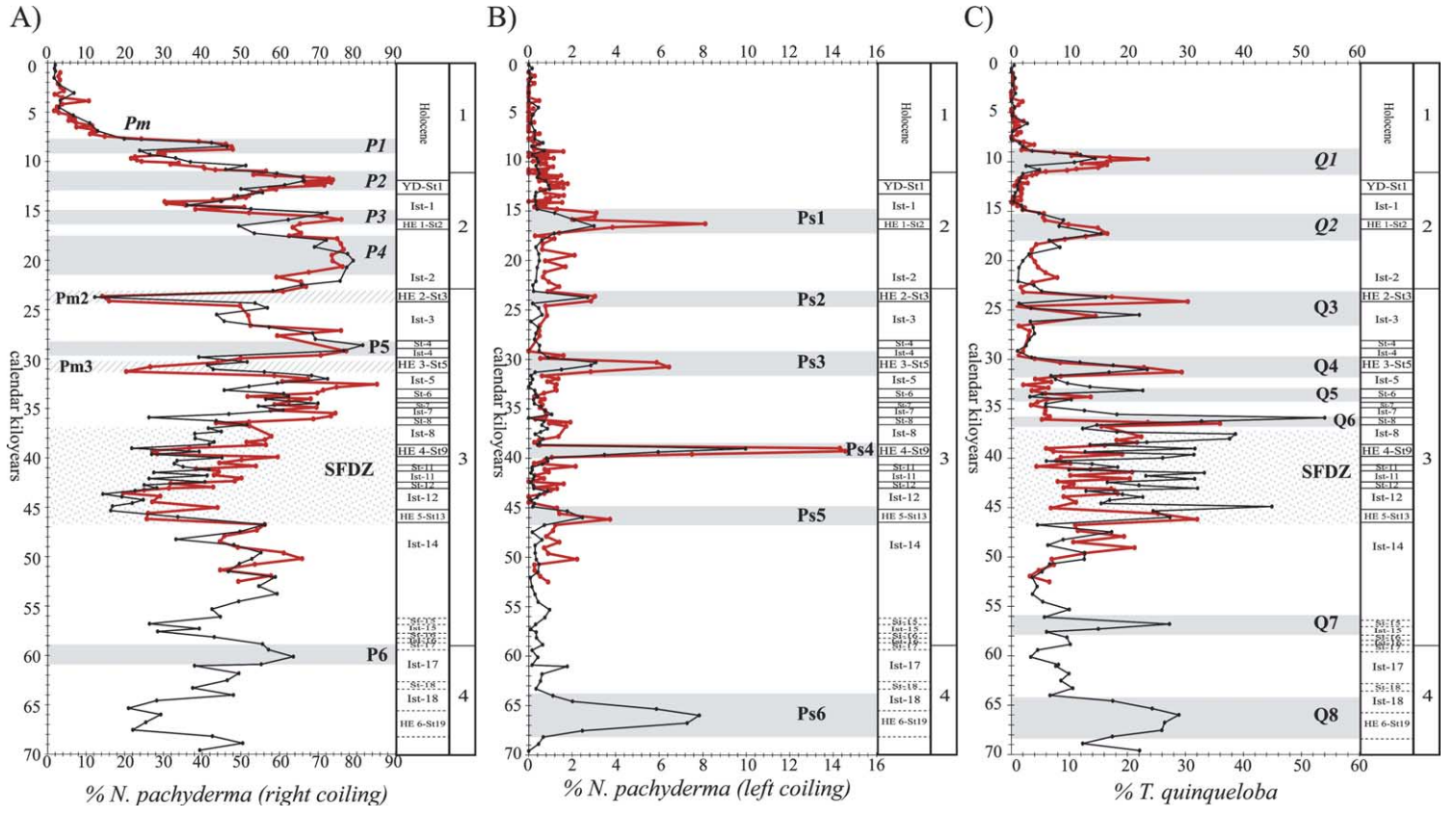

Fig. 4. Quantitative variations of planktonic foraminifera assemblages in cores MD95-2043 (red line) and ODP 977 (black line). The columns at the right of the figure show the different stadials (St) and interstadials (Ist) of the D–O events, together with HEs, and the different isotopic stages. From St-13 downward, the different St and Ist are marked in dashed lines owing to the reduced age control below 54 kyr in core ODP 977 (see text). The different zones identified in the cores are delimited by solid grey bands (maxima in abundance), striped ones (minima in abundance), or only by name (bio-events). Pujol and Vergnaud-Grazzini (1989) events are in italics. Abbreviation: SFDZ, Small Foraminifera Dominance Zone. (A) *Neogloboquadrina pachyderma* (right coiling). (B) *N. pachyderma* (left coiling). (C) *Turborotalita quinqueloba*. (D) *Globorotalia scitula*. (E) *Globorotalia inflata*. (F) *Globigerina bulloides*. (G) *Globigerinoides ruber* white. (G) *G. ruber* pink.

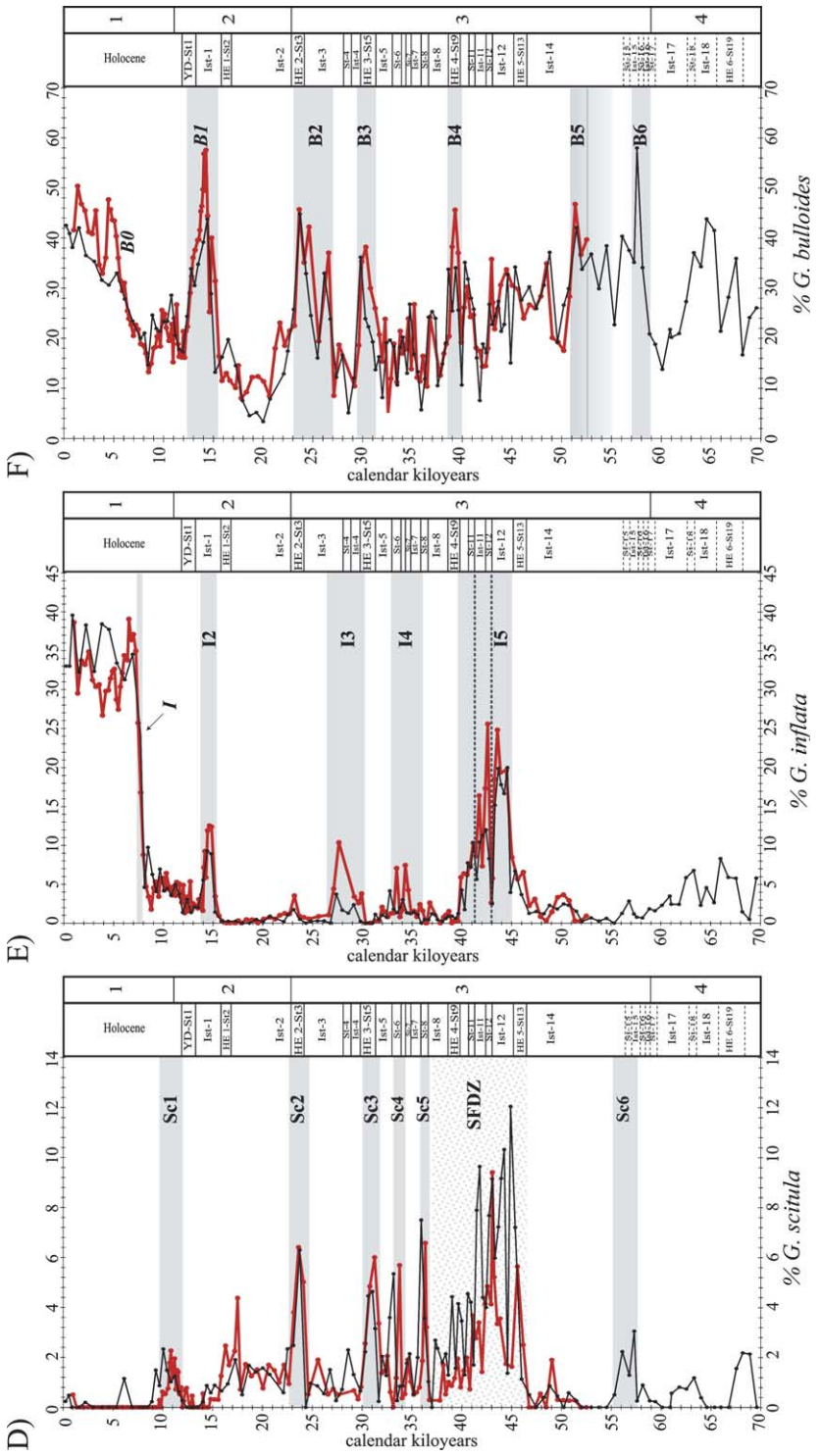

Fig. 4 (*Continued*).

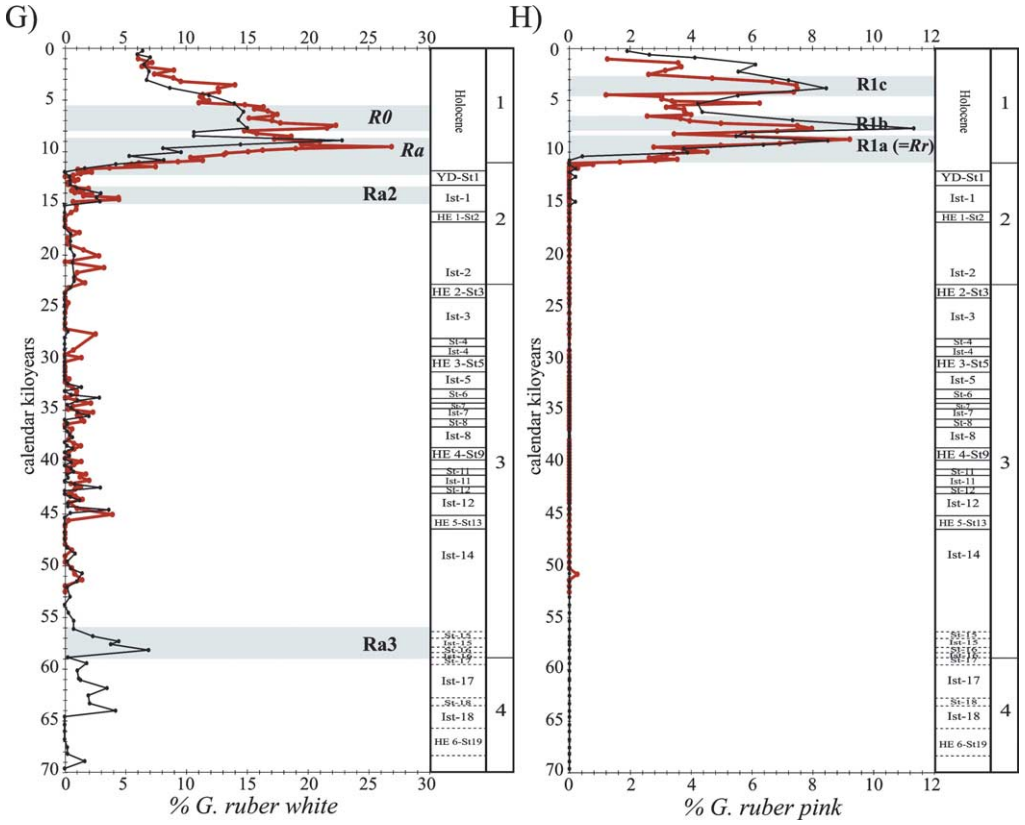

Fig. 4 (*Continued*).

the first five HEs in core MD94-2043. These were recognised as significant decreases in SSTs and sharp increases in the polar species *N. pachyderma* l.c. In core ODP 977, these influxes of *N. pachyderma* l.c. also appear and were used to locate the HEs (Fig. 3b). Since HE6 is only recorded in core 977, we gave it an average age based on the different ages provided for this event in the North Atlantic and Mediterranean (Bond et al., 1992, 1993; Grousset et al., 1993; Lebreiro et al., 1996; Manighetti et al., 1995; Paterne et al., 1999; Chapman and Shackleton, 1998; van Kreveld et al., 1996; Cayre et al., 1999; see Table 1).

HEs are linked with maximum cooling during the rapid climatic fluctuations defined in ice cores from Greenland (Dansgaard et al., 1993; Grootes et al., 1993), known as D–O cycles (Bond et al., 1993). These variations in atmospheric temperature over Greenland have been linked to changes in surface temperature of the waters of the Alboran Sea (Cacho et al., 1999; Fig. 3c). In the SST curve of core MD95-2043, obtained with the alkenone technique, it is thus possible to identify the last 13 D–O cycles (Cacho et al., 1999). This correlation (Fig. 3c) serves as a basis for identifying the relationships between these D–O events and the faunal variations in the cores (Fig. 4).

It should be stressed that the age model of ODP 977 is well established up to 54 kyr (since it is essentially based on the correlation with core MD95-2043) whereas up to 70 kyr there may be some uncertainties in the age model. This is why in Fig. 4 and Table 2 the D–O events below 54 kyr are only shown by a dotted line.

According to our age model, an average time resolution of 510 yr per sample is obtained for the ODP 977 core. The temporal resolution for core MD95-2043 is 320 yr per sample.

Table 2
Planktonic foraminifera events and their relation with D–O stadials and interstadials

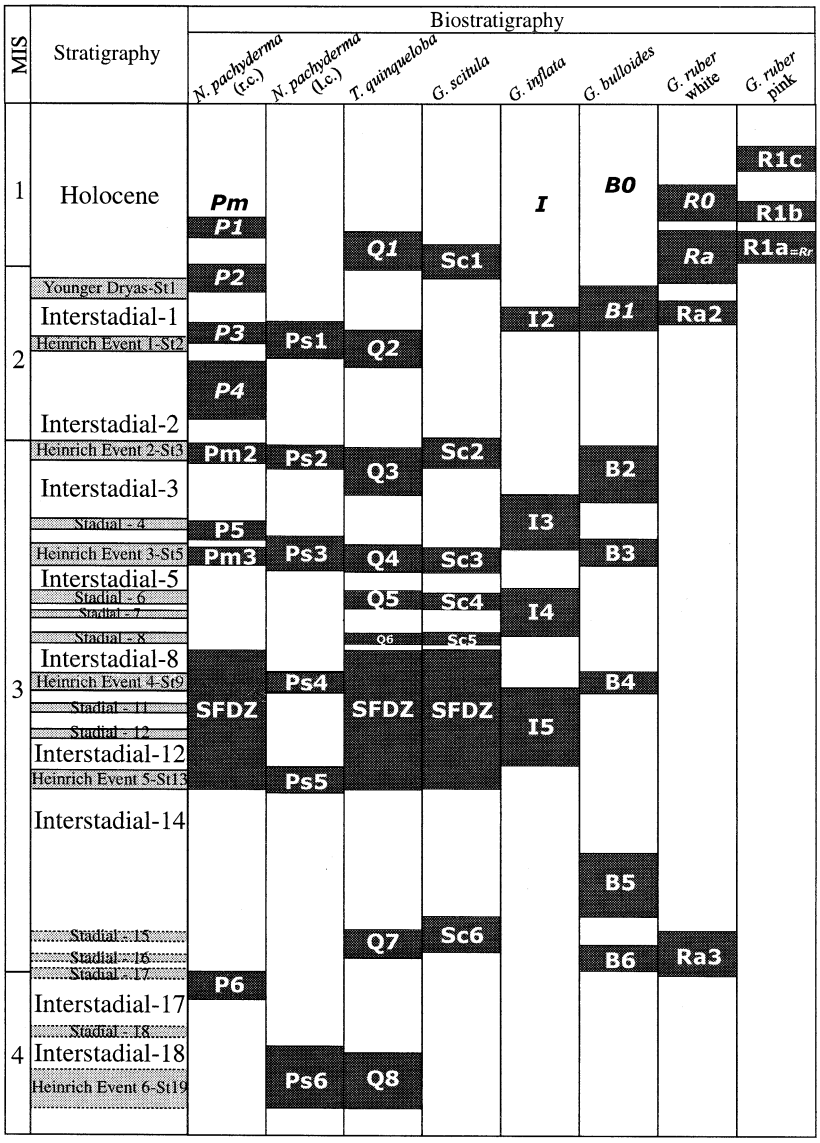

Light grey bands in the stratigraphy correspond with cold stadials, and white ones with warm interstadials. Pujol and Vergnaud-Grazzini (1989) events are in italics.

4. Results

4.1. High resolution planktonic foraminifera biostratigraphy in the Alboran Sea during the last glacial–interglacial period

By studying the variations in the associations of planktonic foraminifera in the westernmost part of the Mediterranean Sea, we were able to identify up to 48 biological events in the last 70 kyr, of which 29 are newly defined (Fig. 4A–H).

Around 22 species were found in each core, although if the varieties and different coiling types are included this number rises to 26. The dextral

and sinistral coilings of *Globorotalia truncatulinoides*, *Globorotalia scitula* and *Neogloboquadrina pachyderma* were considered, together with the white and pink varieties of *Globigerinoides ruber*. The group known as '*N. pachyderma–N. dutertrei* integrade' was also included.

The current association in the Alboran Sea, deduced from the coretops, mainly comprises *Globigerina bulloides* and *Globorotalia inflata*. The first of these is the most abundant today (more than 40%) and together they represent more than 70% of the association. *Globigerinoides ruber* white, a species from warmer habitats (tropical and subtropical), may represent up to 17% of the association. The rest of the species appear with lower percentages.

Based on previous studies by Pujol and Vergnaud-Grazzini (1989), and going farther back in time, we identified a series of characteristic changes in the most important species of planktonic foraminifera. Following the nomenclature introduced by Pujol and Vergnaud-Grazzini (1989) for each species, we identified zones defining intervals of time in which certain species reach values well above or well below the average. The upper or lower limits of these zones are marked by sharp changes in abundance that can be used to define the true bio-events.

To define the age intervals in which each faunal event occurred, as a reference we always used the variations in the taxa in core MD95-2043, the age model of which is best established. Exceptions are those events that occurred between 54 and 70 kyr, which only appear in core ODP 977, for which we used the age model of this core. All the events can be seen in Tables 2 and 3, and in Fig. 4.

4.1.1. Neogloboquadrina pachyderma *right coiling*

At present, this subpolar species is not very abundant (3%), but the mean of the last 70 kyr reaches 43% of the fossil assemblage, being one of the principal species of the planktonic foraminifera association. This mean is punctuated by several characteristic maxima and minima, which we used to define a series of zones. The maximum values (higher than 80%) are reached in the Last Glacial Maximum (LGM) and the minimum values in the Upper Holocene.

Pujol and Vergnaud-Grazzini (1989) defined four major zones: maxima P1, P2, P3 and P4 and the minimum of the Holocene (bio-event Pm). All of them can be recognised in the two cores (Fig. 4A), and another four zones – two of high abundance (P5 and P6) and two of low abundance (Pm2 and Pm3) – were identified (Tables 2 and 3; Fig. 4A). To delimit the age of occurrence of zone P6, we used core ODP 977 since it is the only one in which it is recorded (Fig. 4). The decrease in abundance of this species during the Holocene (bio-event Pm) is a remarkable event that occurred at 7.7 kyr, coinciding with *Globorotalia inflata* bio-event I.

4.1.2. Neogloboquadrina pachyderma *left coiling*

The mean abundance of this small polar species is very low in the record (1.15% in MD95-2043 and 0.84% in ODP 977), although it displays some short and prominent influxes that may reach as high as 14.5% in MD95-2043 and almost 10% in ODP 977, which occurred during HEs (Cacho et al., 1999). Thus, we define zones Ps1 to Ps5 in core MD95-2043 and zones Ps1 to Ps6 in core ODP 977 (Fig. 4B; Tables 2 and 3). In both cores, the maximum abundance is reached in zone Ps4.

4.1.3. Turborotalita quinqueloba

This small subpolar species (Bé, 1977) is very rare in modern samples and becomes common in the Alboran Sea at 7.7 kyr. Its mean abundance is not very high (11.41% in ODP 977 and 7.39% in MD95-2043), although it may represent the principal component of the assemblage in some of the events defined (Fig. 4C). Zones Q1 and Q2, defined by Pujol and Vergnaud-Grazzini (1989), were identified and, going back in time, we define zones Q3–Q8 (Fig. 4C).

Zone Q5 was recognised by a maximum in abundance that occurred at 33.8 kyr in MD95-2043, and at 33.2 kyr in ODP 977. This offset is due to small errors in the age model, since a constant sedimentation rate between the control points was assumed, which is not always necessarily the case. The same is true for the maximum in zone Q6, which in ODP 977 may represent more than 50% of the association of planktonic foraminifera. The maximum abundance of this species

Table 3
Calendar ages (in kyr) of all planktonic foraminifera zones identified in cores MD 95-2043 and ODP 977

N. pachyderma r.c. zones (figure 4A)		
Pm **bioevent**		7.7
P1	Top	7.7
	Max.	8.8
	Bottom	9.2
P2	Top	10.8
	Max.	11.8
	Bottom	13.1
P3	Top	15.2
	Max.	15.8
	Bottom	16.7
P4	Top	17.3
	Max.	18.9
	Bottom	21.7
Pm2	Top	23.2
	Bottom	24.6
P5	Top	28.1
	Max.	29.1
	Bottom	29.7
Pm3	Top	30.2
	Bottom	31.3
SFDZ	Top	36.7
	Bottom	46.7
P6	Top	58.1
	Max.	60.1
	Bottom	61.0

N. pachyderma l.c. zones (figure 4B)		
Ps1	Top	14.6
	Max.	16.2
	Bottom	17.5
Ps2	Top	23.2
	Max.	23.6
	Bottom	24.6
Ps3	Top	29.2
	Max.	30.8
	Bottom	31.7
Ps4	Top	38.4
	Max.	39.3
	Bottom	40.5
Ps5	Top	44.4
	Max.	46.2
	Bottom	46.7
Ps6	Top	63.3
	Max.	66.0
	Bottom	69.6

T.quinqueloba zones (figure 4C)		
Q1	Top	6.7
	Max.	9.7
	Bottom	11.4
Q2	Top	14.8
	Max.	17.2
	Bottom	18.3
Q3	Top	23.2
	Max.	24.1
	Bottom	26.6
Q4	Top	29.6
	Max.	31.3
	Bottom	32.0
Q5	Top	33.1
	Max.	33.8
	Bottom	34.6
Q6	Top	35.7
	Max.	36.4
	Bottom	36.6
SFDZ	Top	36.7
	Bottom	46.7
Q7	Top	56.1
	Max.	56.8
	Bottom	57.6
Q8	Top	64.0
	Max.	66.0
	Bottom	68.2

G. scitula zones (figure 4D)		
Sc1	Top	9.5
	Max.	10.8
	Bottom	11.9
Sc2	Top	22.7
	Max.	23.6
	Bottom	24.6
Sc3	Top	29.6
	Max.	31.3
	Bottom	32.0
Sc4	Top	33.1
	Max.	33.8
	Bottom	34.0
Sc5	Top	35.2
	Max.	36.4
	Bottom	36.6
SFDZ	Top	36.7
	Bottom	46.7
Sc6	Top	55.3
	Max.	57.3
	Bottom	57.6

G. inflata zones (figure 4E)		
I **bioevent**		7.7
I2	Top	13.9
	Max.	14.6
	Bottom	15.8
I3	Top	26.6
	Max.	27.6
	Bottom	30.3
I4	Top	33.1
	Max.	34.3
	Bottom	36.1
I5	Top	39.6
	Max.	42.6
	Bottom	45.0

G. bulloides zones (figure 4F)		
B0 **bioevent**		5.6
B1	Top	12.4
	Max.	14.3
	Bottom	15.6
B2	Top	23.0
	Max.	23.6
	Bottom	27.0
B3	Top	29.2
	Max.	30.3
	Bottom	31.9
B4	Top	37.8
	Max.	39.3
	Bottom	39.9
B5	Top	50.2
	Max.	51.3
	Bottom	52.5
B6	Top	57.2
	Max.	57.6
	Bottom	58.9

G. ruber white zones (figure 4G)		
R0	Top	5.3
	Max.	7.7
	Bottom	8.0
Ra	Top	8.8
	Max.	9.5
	Bottom	12.3
Ra2	Top	13.1
	Max.	14.6
	Bottom	14.8
Ra3	Top	56.1
	Max.	58.1
	Bottom	58.8

G. ruber pink zones (figure 4H)		
R1c	Top	2.5
	Max.	3.9
	Bottom	4.4
R1b	Top	6.5
	Max.	7.7
	Bottom	8.0
R1a (=*Rr*)	Top	8.5
	Max.	8.7
	Bottom	10.9

Pujol and Vergnaud-Grazzini (1989) events are in italics.

A)

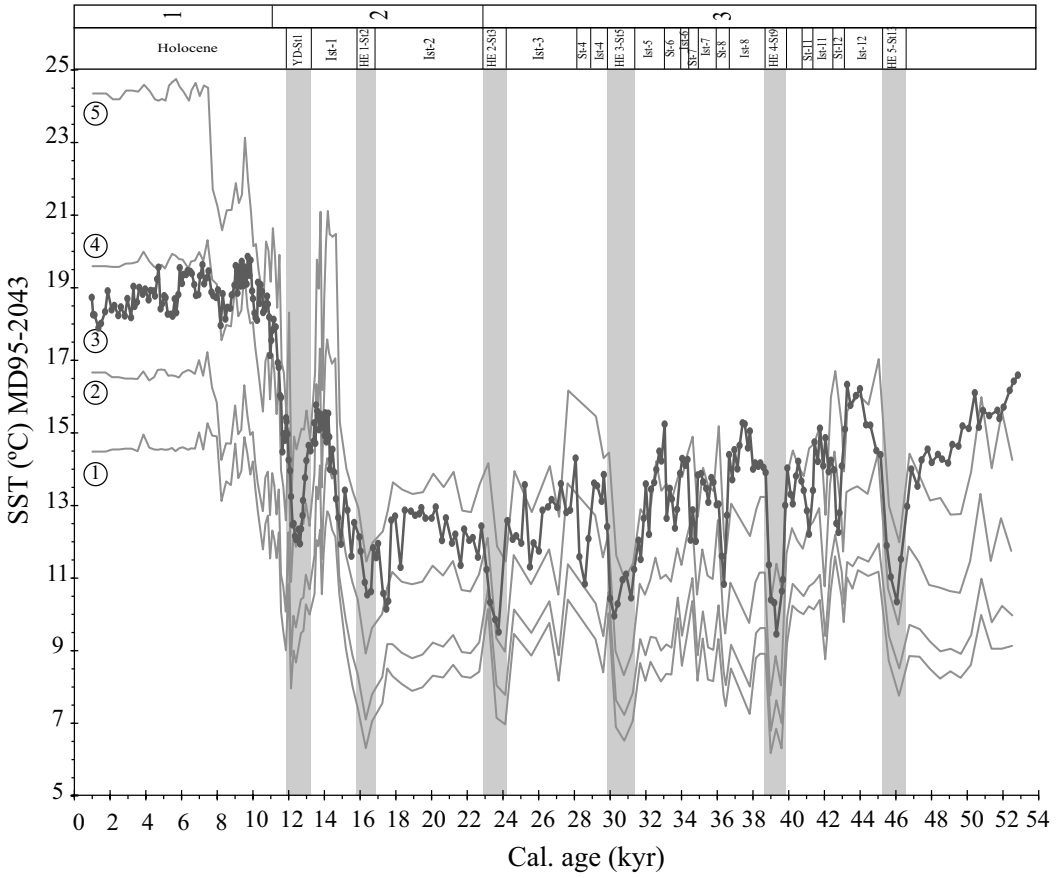
1
2
3
Holocene
YD-St1
Ist-1
HE 1-St2
Ist-2
HE 2-St3
Ist-3
St-4
Ist-4
HE 3-St5
Ist-5
St-6
St-7
Ist-7
St-8
Ist-8
HE 4-St9
St-11
Ist-11
St-12
Ist-12
HE 5-St13
SST (ºC) MD95-2043
Cal. age (kyr)
① ② ③ ④ ⑤

B)

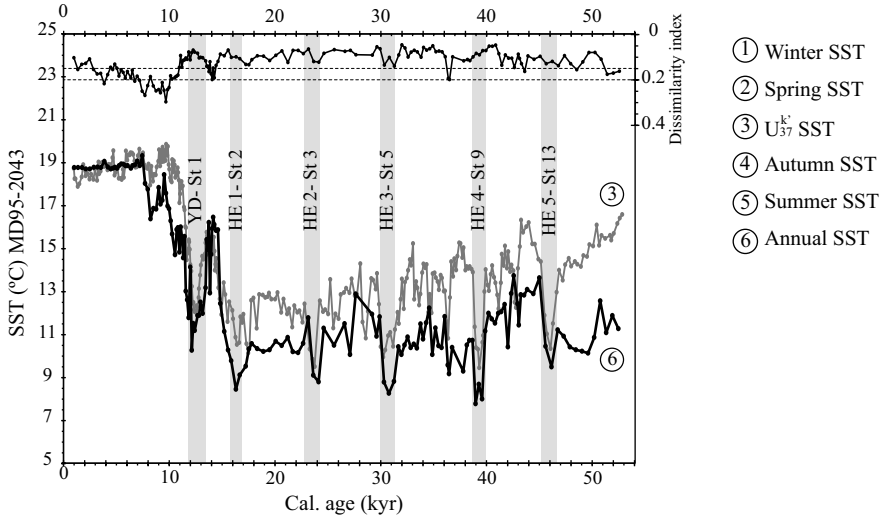
SST (ºC) MD95-2043
Dissimilarity index
Cal. age (kyr)
YD- St 1
HE 1 - St 2
HE 2 - St 3
HE 3 - St 5
HE 4 - St 9
HE 5 - St 13
① Winter SST
② Spring SST
③ $U^{k'}_{37}$ SST
④ Autumn SST
⑤ Summer SST
⑥ Annual SST

Table 4
Results of PCA carried out on ODP 977 samples

Species/factor load	Factor 1	Factor 2	Factor 3	Factor 4	Factor 5
O. universa	0.006	0.024	−0.001	0.001	0.073
G. ruber rosea	−0.009	0.085	0.003	0.061	**0.143**
G. ruber alba	−0.045	0.169	0.019	0.176	**0.946**
G. trilobus	−0.005	0.006	0.003	0.003	0.046
G. sacculifer	−0.002	0.002	0.001	0.000	0.014
G. bulloides	−0.053	**0.366**	−0.078	**−0.919**	0.105
T. quinqueloba	−0.137	−0.088	**−0.959**	0.051	0.008
N. pachyderma (*l.c.*)	−0.006	−0.008	−0.041	−0.009	0.001
N. pachyderma (*r.c.*)	**0.988**	0.008	−0.139	−0.036	0.054
G. inflata	0.010	**0.904**	−0.056	0.337	−0.239
G. scitula	−0.019	0.022	**−0.156**	0.042	−0.004
G. glutinata	0.001	0.033	**−0.152**	0.038	−0.004
Variance (%)	56.45	10.76	12.20	16.45	3.72
Accumulated variance (%)	56.45	62.22	79.42	95.87	99.60

recorded in zone Q8, at 66 kyr, is coeval with zone Ps6 (Fig. 4C; Table 3).

4.1.4. Globorotalia scitula

This globorotalid is not very abundant in the cores; the maxima hardly surpass 12 and 9% of the assemblage (in ODP 977 and MD95-2043, respectively) and the average ranges around 1.4%. *G. scitula* disappears from MD95-2043 at 9.5 kyr, but in core ODP 977 this disappearance occurs slightly later, at 8.4 kyr (Fig. 4D).

Zones Sc4 and Sc5 occur close to zones Q5 and Q6 (Fig. 4; Tables 2 and 3), and the small discrepancies between both cores are due to minor errors in the age model.

4.1.5. *Small Foraminifera Dominance Zone*

This is an interval of 10 kyr that we have called the 'Small Foraminifera Dominance Zone' (SFDZ) because the assemblage is dominated by small species such as *Turborotalita quinqueloba* and *Globigerinita glutinata*, accompanied by a high percentage of *Globorotalia scitula*. This zone ranges between 36.7 and 46.7 kyr (Table 3), within MIS 3, and is characterised by sharp fluctuations in the abundance of the dominant species (Fig. 4). *Neogloboquadrina pachyderma* (right coiling, r.c.) tends to decrease while *G. scitula* increases in abundance along the zone, and *T. quinqueloba* fluctuates around 14% in MD95-2043 and 22% in ODP 977 (Fig. 4). The limits of the zone (36.7 and 46.7 kyr) are fairly precise and coincide in all three taxa and in both cores (Table 3).

4.1.6. Globorotalia inflata

The current abundance of this species is very significant in the Alboran Sea today (more than 30% of the association). It has been a significant component of the foraminiferal assemblage since 7.7 kyr ago, when it replaced *Neogloboquadrina pachyderma* (r.c.), which decreased sharply at that time. This change has already been reported by Pujol and Vergnaud-Grazzini (1989) as event I. During the last glaciation *G. inflata* is rare. However, at certain times (zones I2 to I5) the species is relatively abundant (Tables 2 and 3; Fig. 4E). Zone I5 contains several significant minima at 42.9 and 42 kyr (Fig. 4E).

4.1.7. Globigerina bulloides

This is the dominant species in current associations, reaching around 40% in both coretops,

Fig. 5. Palaeotemperatures obtained with the MAT, and comparison with $U^{k'}_{37}$ SST in core MD95-2043. (A) Seasonal palaeo-SST (thin lines) and alkenone SST (thick line). Winter correspond to the February temperature, Spring is the April–May mean, Autumn is the October–November mean, and Summer is the August temperature. (B) Comparison between the $U^{k'}_{37}$ SST record (grey line) and MAT annual mean SST record (black line). The dissimilarity index of MAT reconstructions is also shown.

although the maxima (about 58%) are recorded at 14 kyr in MD95-2043 and at 57.6 kyr in ODP 977 (zone B6). Events B0 and B1, defined by Pujol and Vergnaud-Grazzini (1989), appear in both cores and are the starting points for the definition of zones B2, B3, B4, B5 and B6 (Fig. 4F).

In the Late Holocene, the significant rise in *G. bulloides* occurring at 5.6 kyr defined bio-event B0, the age of which coincides with that reported by Pujol and Vergnaud-Grazzini (1989). However, the age of 13 kyr reported by these authors for event B1 is slightly younger than that obtained in this work. These chronological discrepancies may be due to the different resolutions of the two studies. In zone B2 there are two small minima at 24.1 and 25.6 kyr (see Fig. 4F). Zone B5 is recorded towards the base of the interval studied in core MD95-2043, although according to the ODP 977 record its extent may be greater (Fig. 4F).

4.1.8. Globigerinoides ruber *white*

This species, which normally appears in warm waters (Bé, 1977; Hemleben et al., 1989), is frequent in the Holocene but decreases in abundance at 12 kyr. Pujol and Vergnaud-Grazzini (1989) defined two events (R0 and Ra). The maximum abundance of this species observed within zone R0 is coeval with the sharp decrease in *Globorotalia inflata*, (event I), as reported by Pujol and Vergnaud-Grazzini (1989). Below event Ra, we define the Ra2 and Ra3 zones, the latter only in core ODP 977 (Tables 2 and 3; Fig. 4G). In the SFDZ, sharp variations of up to 3% in *G. ruber* white can be observed, (Fig. 4G).

4.1.9. Globigerinoides ruber *pink*

This pink variety is less abundant than the white one and usually thrives in warmer waters. It is only present during the Holocene, disappearing at 11.2 kyr in MD95-2043 and at 10.4 kyr in Site 977. Its abundance is always low, never reaching 12%. Pujol and Vergnaud-Grazzini (1989) define Rr as the first local occurrence of *G. ruber* pink. We maintain this definition, although we employ a slightly different terminology, using the term R1 to refer to Rr; R1b to refer to the maximum values following it, and R1c to refer to the last maximum reached in the Late Holocene (Tables 2 and 3; Fig. 4H).

Between zones R1b and R1a (Fig. 4H), at 8.2 kyr, there is a more or less sharp minimum, which coincides with the minimum between zones Ra and R0 (Fig. 4G).

4.2. Palaeotemperature reconstruction in core MD95-2043

The SST reconstruction carried out in core MD95-2043 with the MAT (Fig. 5) based on the analysis of the foraminiferal assemblages allowed us to obtain temperature estimations for the different seasons and compare these results with those derived from the alkenone record (Cacho et al., 1999). The mean errors are: ±1.58°C for winter temperatures; ±1.66°C for spring data; higher for summer results (±2.26°C), and ±1.92 for autumn values.

For the last 8 kyr, the temperatures obtained with the $U^{k'}_{37}$ and MAT methods are very stable. The coretop SST estimations for the different seasons (14.5°C for winter, 16.6°C for spring, 24.4°C for summer and 19.6°C for autumn) correspond closely to the Recent temperatures in this region (14.6°C for winter, 16.8°C for spring, 24.3°C for summer and 19.7°C for autumn; Levitus, 1982). The $U^{k'}_{37}$ SST estimation for the coretop is 18.8°C; a temperature between modern spring and autumn SSTs (Fig. 5). The seasonal gradient (the average difference between summer and winter temperatures) during the last 8 kyr is around 10°C (Fig. 5), which is very similar to that existing today.

The full glacial–late interglacial temperature contrast is also much higher in the summer temperatures, which decreased more (12°C) than winter temperatures (8°C); the same glacial–interglacial difference is 9°C in the $U^{k'}_{37}$ record. Seasonality during the last glacial is on average 5°C, in contrast to the difference of 10°C observed today and for the last 8 kyr in the Alboran Sea. This reduced seasonality was mainly due to the cooler summer temperatures during the glacial period (Fig. 5).

During the last glacial (MIS 2 and 3), the temperature record points to five prominent cooling

events corresponding to HE1 to HE5. Sea surface temperatures estimated with the MAT are very similar for all Heinrich events, reaching values of around 7°C for the winter seasons, which is well below the 9–10°C estimated by the alkenone method. HE4 is the coldest (below 7°C) and HE5 the warmest (around 8°C).

4.3. Planktonic foraminifera assemblages in ODP 977 core samples

The five factors resulting from PCA analysis of the ODP 977 samples (Table 4) explain 99.6% of the total variance of the sample. The first and most important factor (factor 1) accounts for 56.5% of the variance and is represented by the species *Neogloboquadrina pachyderma* (r.c.). Factors 3 and 4 together account for 30% of the variance and are controlled by *Turborotalita quinqueloba*, *Globorotalia scitula* and *Globigerinita glutinata* (factor 3) and *Globigerina bulloides* (factor 4). Factors 2 and 5 explain about 15% of the total variance and have high loadings in the species *Globorotalia inflata* (factor 2) and *Globigerinoides ruber* white and *G. ruber* pink (factor 5). Fig. 6 shows the plot of the three groups of species deduced. Factors 1 and 3 reach the highest values during glacial times (MIS 2, 3 and part of 4) but decrease during the Holocene and some of the warmer interstadials, when factors 2 (*G. inflata*) and 5 (*G. ruber*) increase (Fig. 6). By contrast, factor 4 (*G. bulloides*) is significant both during glacial and interglacial times.

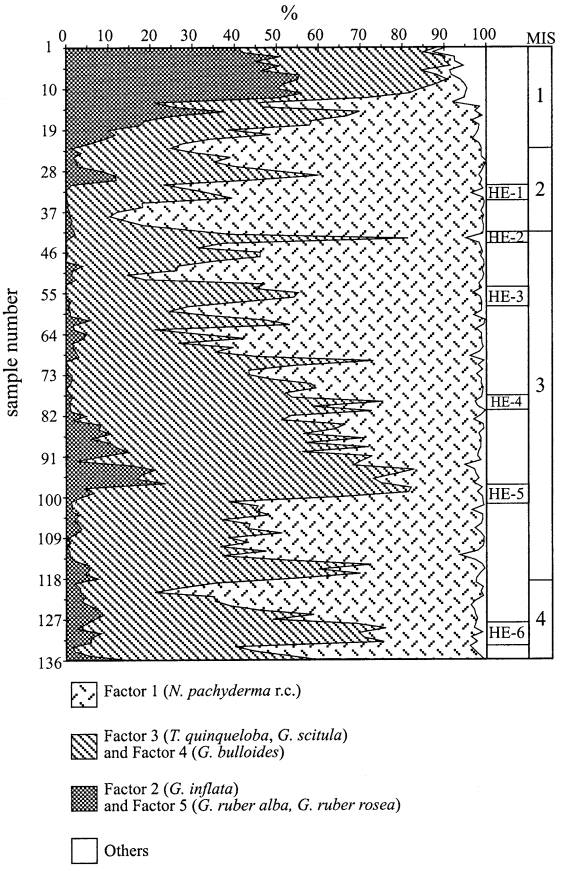

Fig. 6. Percentage of different factors derived from PCA carried out on core ODP 977. The factors were associated according to the ecological requirements of the species characterising them.

5. Discussion

5.1. Biostratigraphic correlation with other areas in the Mediterranean

We identified all the bio-events and phases or ecozones recognised by Pujol and Vergnaud-Grazzini (1989) over the past 18 kyr, although the order of the bio-events (in 'phase 5' and 'phase 4') is slightly different since zone Q1 occurs before the events of *Globigerinoides ruber* (Rr and Ra), whereas Pujol and Vergnaud-Grazzini (1989) recorded the opposite (first Ra and Rr and then zone Q1; table IV, p. 167). In any case, the resolution of their study was considerably more limited than in the present one, which could affect the ages of the tops and bases of the zones.

Other authors (e.g. Sbaffi et al., 2001; Capotondi et al., 1999; Hayes et al., 1999; Jorissen et al., 1993) have analysed the biostratigraphy of the last glacial–interglacial transition in the Mediterranean.

Capotondi et al. (1999) established ten ecozones for the last 23 kyr in the Tyrrhenian Sea and eight in the Adriatic Sea (last 15 kyr) based on the study of the distribution of planktonic foraminifera in 60 cores. Direct comparison with our own results is difficult because Capotondi et al. (1999) carried out semi-quantitative analyses of the

>63-μm fraction, which – in particular – could increase the abundance of small species such as *Turborotalita quinqueloba* or *Globigerinita glutinata*. However, some of the faunal variations used to define each ecozone can be identified here. Ecozones 9 and 10 of Capotondi et al. (1999) can be correlated with HE1 and HE2. Concerning the other ecozones, it is only possible to compare some faunal variations that are similar in both records, such as the increase in *Neogloboquadrina pachyderma* (r.c.) during the YD (zone P2), or the rapid increase in both varieties of *Globigerinoides ruber* (zones Ra and R1a) during the Termination Ib (T1b). At this moment, the Recent fauna appears, being different in the Alboran Sea and in the Tyrrhenian and Adriatic (Capotondi et al., 1999). The Recent fauna of the Alboran Sea, characterised by high percentages of *Globorotalia inflata* and low values of *N. pachyderma* r.c., developed at 7.7 kyr, linked to the establishment of the oceanographic fronts associated with the semi-permanent anticyclonic gyres (Rohling et al., 1995).

Jorissen et al. (1993) divided the Late Pleistocene–Holocene of the Adriatic Sea succession into three zones on the basis of the frequencies of the planktonic fauna (Zones I, II and III). The limits between these zones, which approximately coincide with Terminations Ia (the II/III limit) and Ib (the I/II limit), can also be recognised in our cores. The limit between zones II and III is situated before Sc1 (Fig. 4D) and the limit between zones I and II would be situated close to the Ra zone (Fig. 4G), at 9.5 kyr, preceding an increase in the SPRUDTS group (*Globigerinella siphonifera*, *Hastigerina pelagica*, *Globigerina rubescens*, *Orbulina universa*, *Globigerina digitata*, *Globigerinoides tenellus* and *Globigerinoides sacculifer*; Jorissen et al., 1993).

In a recent work by Sbaffi et al. (2001), the authors distinguish nine 'association biozones' in the Tyrrhenian Sea over the past 34 kyr. The authors define the biozones on the basis of the appearance or disappearance of specific taxa, such that it is possible to establish a direct comparison between these 'association biozones' of the Tyrrhenian Sea and our own biological events in the Alboran Sea. Most of the changes in the Tyrrhenian fauna can be identified in the westernmost Mediterranean, with the exception of certain specific changes such as the increase in *Globigerinoides ruber* white during Interstadial D–O 5 (Biozone 9 of Sbaffi et al., 2001), or the decrease in *Globorotalia inflata* in the Holocene (Biozone 2), which do not appear in our cores. These authors record the disappearance of *Globorotalia scitula* in Biozone 3, at about 11 kyr. The diachronism in the disappearance of this species in the western Mediterranean, proposed by Hayes et al. (1999), is confirmed by our data, since *G. scitula* first disappears at 9.5 kyr in core MD95-2043 and, shortly afterwards, at 8.4 kyr in core ODP 977, although in the latter it re-appears at 6.1 kyr.

Hayes et al. (1999) stated that the planktonic foraminifera biostratigraphy may be a useful tool, although – in some cases – only at a local scale. While some of the faunal changes, such as those affecting *Globigerinoides ruber*, *Globorotalia scitula*, the SPRUDTS group, etc. (Jorissen et al., 1993; Hayes et al., 1999; Capotondi et al., 1999; Pujol and Vergnaud-Grazzini, 1989; Sbaffi et al., 2001; this study), were synchronous in the central and western Mediterranean, other taxa such as the neogloboquadrinids, or *Globorotalia inflata* and *Turborotalita quinqueloba* followed an abundance distribution pattern that was related to the regional climatic and hydrographic characteristics of the Mediterranean sub-basin in which they developed.

PCA Factors 1 (*N. pachyderma* r.c.), 3 (*Turborotalita quinqueloba*, *Globorotalia scitula*) and 4 (*Globigerina bulloides*) are linked to the subpolar planktonic foraminifera assemblage, while the other two factors (factor 2, *Globorotalia inflata* and factor 5, *Globigerinoides ruber*) are undoubtedly related to the transitional and subtropical assemblages in the Atlantic Ocean (Bé, 1977; Hemleben et al., 1989).

5.2. Seasonal palaeotemperatures in the Alboran Sea and their relationship with $U^{k'}_{37}$ palaeo-SST

Analysis of the relative composition of C-37 unsaturated alkenones ($U^{k'}_{37}$ index) in core MD95-2043 provided a continuous record of SSTs for the last 54 kyr (Cacho et al., 1999).

Alkenones are long-chain methyl ketones produced by cocolithophoral algae. In the present ocean, the principal producer is thought to be *Emiliania huxleyi* (Volkman et al., 1980) and therefore the quality of the temperature estimations obtained with these organic compounds are undoubtedly controlled by the seasonal production and sedimentation of this coccolith species.

A first short-term cooling event is seen at around 8.2 kyr both in the $U^{k'}_{37}$ and MAT records. This cooling was particularly significant during summer, when a temperature drop of around 4°C occurred. A decrease in abundance of warm-water species *Globigerinoides ruber* (white and pink; Fig. 4G,H), accompanied by an increase in cool-water species *Neogloboquadrina pachyderma* (r.c.) (P1 event; Fig. 4A), are also recorded in this interval. This 8.2-kyr Holocene cooling has been broadly recognised in Greenland ice core records (Dansgaard et al., 1993; Grootes et al., 1993; Alley et al., 1997) and in additional western Mediterranean cores (Cacho et al., 2001). A second and more prominent cooling event occurred during the Younger Dryas, affecting summer temperatures in particular, which dropped from around 24°C at 8 kyr to 14°C at 12 kyr. This temperature reduction of 10°C contrasts with that seen with the $U^{k'}_{37}$ method (7°C). By contrast, the magnitude of the winter temperature cooling is around 5°C.

As already seen in the alkenone record (Cacho et al., 1999), temperature also fell during the cold D–O stadial events but this drop was less intense, supporting the existence of a mechanism of amplification leading to more severe coolings during the HEs, as already stated by Cacho et al. (1999). Nevertheless, the fact that MAT–SST decrease to similar values (around 7°C) throughout the HE could be representative of a non-analog situation, probably due to the calibration of the data set, despite the low dissimilarities obtained during such events (Fig. 5B). This SST reduction to 7°C during winter is also recorded during HE6 (ODP 977; unpublished data).

The coretop SST estimation provided by the $U^{k'}_{37}$ method is close to the average annual SST for this region, which in turn lies close to the autumn temperatures (Fig. 5B). This situation can be extended down until 8 kyr and during the Bölling–Allerød, where the $U^{k'}_{37}$ SST record lies between the spring and autumn MAT records (Fig. 5). Before 8 kyr, however, the SST record of $U^{k'}_{37}$ is generally slightly or well above the autumn MAT record, approaching or even surpassing summer temperatures during MIS 3. The same is true in ODP 977 (unpublished data). In particular, during some of the most prominent interstadials, such as Ist 8, Ist 12 and Ist 14, the temperatures estimated with the alkenone method are higher than summer temperatures based on foraminiferal counts. Nevertheless, the temperatures of the alkenone record approach the autumn temperatures during most of the HEs. The magnitude of the thermal change between these prominent interstadials and the Stadials of HE5 and HE4 is higher in the $U^{k'}_{37}$ record (4°C; Cacho et al., 1999) than in the MAT average annual record (2.5°C). These changes suggest that seasonal variations in alkenone production may have played a significant role in the $U^{k'}_{37}$ records.

The correspondence between the alkenone SST record and the autumn–spring MAT record for the last 8 kyr, a situation similar to that existing today, may be explained by the present seasonal production and accumulation of *Emiliania huxleyi*, the main alkenone producer, which is mainly concentrated in spring (55%), autumn (21%) and summer (18%), while its winter production is very low (6%) (Bárcena et al., in preparation). However, before 8 kyr, and particularly during MIS 2 and 3 and the most prominent D–O interstadials, a reduction in the relative contribution of winter and spring alkenone export production with respect to its summer and autumn fluxes could have occurred. In any case, further studies would be necessary to better understand the relation between alkenone production and *E. huxleyi* blooms in the Alboran Sea.

In the Tyrrhenian Sea, Sbaffi et al. (2001) made comparisons between MAT and $U^{k'}_{37}$ SST for the last 34 kyr. They observed a relatively close match between the alkenone records and the autumn and spring MAT records, confirming the existence of two coccolith blooms along the year in the central Mediterranean (Sbaffi et al., 2001).

5.3. Response of the planktonic foraminiferal fauna to millennial variability in the Alboran Sea

The strong seasonal contrast between summer and winter temperatures prevailing today in the western Mediterranean and the high inflow volume of Atlantic surface waters lead to strong water stratification during the *non-bloom* regime and to the formation of a deep pycnocline between the MAW and the Mediterranean waters. This favours the growth of symbiont-bearing oligotrophic foraminifera (e.g. *Globigerinoides ruber*), particularly in late summer, while *Globigerina bulloides* proliferates during spring and early summer, when surface waters are fertilised by nutrients advected from the upwelling in the north or through the eddy-induced upwelling along the gyre margin. On the other hand, *Globorotalia inflata* dominates the planktonic assemblage during winter (the *bloom* regime; García-Gorriz and Carr, 2001), in particular along the frontal systems between the Atlantic inflow and Mediterranean waters (Pujol and Vergnaud-Grazzini, 1995; Rohling et al., 1995; Bárcena et al., in preparation).

This planktonic foraminiferal assemblage characteristic of the present hydrographic conditions has prevailed in the Alboran sea from about 8 kyr ago, when *Globorotalia inflata* replaced *Neogloboquadrina pachyderma* (r.c.). Rohling et al. (1995) linked this event to the establishment of the modern front-dominated conditions in the Alboran Sea, when the inflow volume of Atlantic water was close to the present volume. However, before that time the planktonic foraminifera assemblage was dominated by *N. pachyderma* (r.c.), *Globigerina bulloides* and *Turborotalita quinqueloba* (Fig. 4), comprising more than 80% of the association.

The general pattern of abundance of *Neogloboquadrina pachyderma* (r.c.) (Fig. 4A) follows a similar trend to the record of glacial–interglacial SST changes during the last 70 kyr. This trend is similar to the global variation in sea-level (as can be inferred from the $\delta^{18}O$ curve; Fig. 3); the lowest abundances occurred during the Holocene, while maximum percentages were reached at the time of the lowest sea-level, in the LGM. Throughout MIS 3, a downward decrease in abundance is seen. Today, *N. pachyderma* (r.c.) thrives in cool waters ($<12°C$), in particular in oceanographic regions where a shallow nutricline favours the formation of a Deep Chlorophyll Maximum (DCM) (Bé and Tolderlund, 1971; Fairbanks and Wiebe, 1980). At present, these conditions do not occur in the Alboran Sea (Parrilla and Kinder, 1987) because the pycnocline is located at 150–200 m water depth, which is the base of the Atlantic inflowing waters, well below the euphotic layer (Fig. 2). However, this species is currently abundant in the Gulf of Lions in late winter (Pujol and Vergnaud-Grazzini, 1995; Rohling et al., 1995), when the pycnocline rises, facilitating the advection of nutrients into the euphotic zone. Moreover, Alboran Sea winter temperatures reach 14.5°C, whereas in the Gulf of Lions, winter temperatures only reach 12.5°C, nearer the neogloboquadrinid temperature threshold.

However, during the LGM sea-level was on average some 120 m lower than today (Fairbanks, 1989) and the temperature of the Alboran Sea was between 6.5 and 10°C lower than in the Late Holocene (Fig. 5). Because the threshold of Gibraltar has a depth of less than 300 m (Bryden and Kinder, 1991), a lowering of the sea-level by 120 m would have reduced the Atlantic inflow (Rohling and Bryden, 1994), with the subsequent rising of the thermo-nutricline, represented by the interface between the MAW and the MOW. This shallower nutricline, particularly during winter (the *bloom* season), could have favoured the development of *Neogloboquadrina pachyderma* (r.c.) instead of *Globorotalia inflata*, which also grows in that season. Furthermore, the cooling of surface waters during summer and the lower temperature gradient between surface Atlantic waters and the intermediate Mediterranean waters would have resulted in a weaker pycnocline, increasing the vertical mixing and the advection of nutrients into the euphotic layer (Rohling et al., 1995).

Globorotalia inflata, currently linked to the Atlantic inflow jet in the Alboran Sea, has been a significant component of the foraminiferal assemblage in the late Holocene, the Bölling–Allerød, and during substage 3.1, which are time-periods characterised by significant decreases in *Neoglobo-*

quadrina pachyderma (r.c.). The relatively global high sea-levels during these times suggest that these events were associated with higher inflow volumes of Atlantic waters and warmer surface water temperatures in the Alboran Sea.

Besides the glacial to interglacial changes, millennial climatic variability also had a strong impact on the foraminiferal assemblages in the Alboran Sea, particularly during the HEs. These events, which have been identified in the North Atlantic through the presence of IRD or geochemical markers (Bond et al., 1992, 1993; Grousset et al., 1993), were recognised here by prominent influxes in *Neogloboquadrina pachyderma* (l.c.) (Ps1–Ps6) (see also Rohling et al., 1998; Cacho et al., 1999). This species has been typically linked to sea ice and polar and subpolar waters, both in the Antarctic and Arctic seas (Hemleben et al., 1989; Bé and Tolderlund, 1971; Reynolds and Thunell, 1986; Dieckmann et al., 1991; Johannessen et al., 1994). The presence of this species during the HE but not during the other stadials, indicates that the optimum oceanographic conditions for this species (e.g. low SST) were only reached at those times.

Although *Neogloboquadrina pachyderma* (r.c.) was typically abundant in glacial times, it decreased significantly during the HE (Fig. 5) (for example in zones Pm2 and Pm3), with the exception of HE1, where it increased (zone P3; Fig. 4A), and was partially replaced by the species grouped in factor 3 (*Turborotalita quinqueloba*, *Globorotalia scitula* and *Globigerinita glutinata*), together with *N. pachyderma* (l.c.) and factor 4 (*Globigerina bulloides*, except in HE1). For example, zones Pm2, Ps2, part of Q3, Sc2 and part of B2 occurred during HE2, while zones Pm3, Ps3, Q4, Sc3 and B3 correspond to HE3 (Fig. 4). During these cold episodes of MIS 3, the winter SST fell to below 7°C (Fig. 5), such that although there was a shallow nutricline the inflow of North Atlantic cool subpolar waters partially inhibited the growth of *N. pachyderma* (r.c.), favouring other species such as *N. pachyderma* l.c or *T. quinqueloba*. Today, *T. quinqueloba* develops in cold, well-mixed surficial waters associated with a certain degree of turbulence (Johannessen et al., 1994). When conditions became milder (interstadials), *N. pachyderma* (r.c.) dominated the fossil association once again.

Very high values of *Turborotalita quinqueloba* are reached in both MD95-2043 and ODP 977 (maximum 54%, 36.4 kyr ago, zone Q6 in ODP 977), mainly in the zone of rapid variations in the SFDZ and, in general, in MIS 3. These rapid fluctuations in the abundance of *T. quinqueloba* (Fig. 4C) are related to the millennial changes of the D–O stadials and interstadials in this period. For MIS 3, Hayes et al. (1999) and Rohling et al. (1998) also recorded high percentages of *T. quinqueloba* in core BC15 in the Gulf of Lyon while Capotondi et al. (1999) found percentages higher than 80% in all their cores for the last 23 kyr, although the latter information is not useful for the present study owing to the difference in sieve mesh size used for the analysis. Sbaffi et al. (2001) found percentages close to 30% in the Tyrrhenian Sea for 32 kyr.

During the D–O stadials not related to HEs, no increases in *Neogloboquadrina pachyderma* (l.c.) can be seen, whereas *Turborotalita quinqueloba* and *Globorotalia scitula* increase (for example, zones Q5 and Sc4 occurring during Stadial 6, and zones Q6 and Sc5 in Stadial 8; Fig. 4C and D) and *N. pachyderma* (r.c.) decreases, although this decrease is not as sharp as during the HEs (Fig. 4A). *Globigerina bulloides* increases during the HEs and during Stadials 11 and 12, and decreases in frequency during the rest of the cold periods (Fig. 4F). This species seems to be linked to the upwelling events occurring during the spring and early summer (the *non-bloom* period; Hemleben et al., 1989; Pujol and Vergnaud-Grazzini, 1995). The cooling of surface waters during summer, together with the shallow position of the base of the MAW and the consequent reduction in vertical density gradients during the HE and cold stadial events, could have caused increase advection of nutrients into the euphotic zone, stimulating the proliferation of *G. bulloides*. By contrast, *Globorotalia inflata* declined in abundance during the HE and some D–O stadials.

Other species, such as *Globigerinoides ruber*, although rare during the glacial period, are sensitive to the D-O events. *G. ruber* white increases relatively – not more than 4% – during the main

interstadials from 5 to 12 (Fig. 4G) and almost disappears during the HEs. *G. ruber* pink was only present in the Alboran Sea during the past 8.5 kyr. The temperatures reached during interstadials were not sufficiently high and/or the conditions of the Mediterranean did not reach sufficient stability for this species to develop.

6. Conclusions

Study of the associations of planktonic foraminifera in two cores obtained in the Alboran Sea (western Mediterranean) provides a continuous record of the faunal changes over the past 70 kyr. A high resolution sampling allowed us to identify and define 48 bio-events, 29 of which are newly defined. These events are defined by sharp changes in the abundance of species such as *Neogloboquadrina pachyderma* (right and left coiling), *Turborotalita quinqueloba*, *Globorotalia scitula*, *Globorotalia inflata*, *Globigerina bulloides* and *Globigerinoides ruber* (white and pink). Moreover, we have recognised an interval of dominance of small foraminifera (the SFDZ), as well as *T. quinqueloba* and *G. scitula*, between 36.7 and 46.7 kyr.

Most of these events are related to the millennial climatic variability and can be easily correlated with the HEs and D–O events recorded in Greenland. During the HEs, *Neogloboquadrina pachyderma* (l.c.), *Turborotalita quinqueloba*, *Globigerina bulloides* and *Globorotalia scitula* increased sharply, whereas others, such as *N. pachyderma* (r.c.), *Globorotalia inflata* and *Globigerinoides ruber*, tended to disappear.

During the other D–O stadials, with the exception of *Neogloboquadrina pachyderma* (l.c.), something similar occurred in the faunal associations of the western Mediterranean. The interstadials are recorded by small increases in *G. ruber alba*, between 32 and 46 kyr.

Over the past 70 kyr, with the exception of the Late Holocene, *Neogloboquadrina pachyderma* (r.c.) has been the main component of the associations of planktonic foraminifera, owing to the shallow position of the interface between Atlantic and Mediterranean waters, linked to the low position of the sea-level at that time. From the LGM up to 7.7 kyr BP, as the sea-level was rising, *N. pachyderma* decreased in abundance until it was replaced by *Globorotalia inflata* and current hydrographic conditions were established in the Alboran Sea. We suggest that a rapid deepening of the nutricline and pycnocline, linked to the interference between the Atlantic inflowing waters and the MOW, could have favoured this replacement.

During the main D–O stadials (including HEs), the presence of cool surface waters with a certain degree of turbulence led the surface species *Turborotalita quinqueloba* and, during HEs, the polar species *Neogloboquadrina pachyderma* (l.c.) to prosper. When SST increased, in the interstadials, *N. pachyderma* (r.c.) again dominated the fossil association.

The MAT method was used to estimate SST over the last 54 kyr, which were compared with the $U^{k'}_{37}$ temperature record. During the last glacial (MIS 2 and 3) five prominent cooling events are recorded, corresponding to the HE1–5. Winter temperatures during the HE were around 7°C, well below the 9–10°C estimated with the alkenone technique. Whereas for the Late Holocene (last 8 kyr), the temperatures obtained by means of the $U^{k'}_{37}$ method are very similar to the MAT autumn and annual mean temperatures, during glacial times, and particularly during MIS 3, the temperatures provided by the $U^{k'}_{37}$ method are close to the summer SST based on MAT estimations. This could be due either to small errors in the two methods used for the estimations or to changes in the seasonal production of alkenones.

Acknowledgements

This work was funded by DGCYT projects PB-98-0288, FEDER 1FD1997-1148 (CLI), and BTE2002-04670, and by the Spanish Government FPI Grant FP96 11964731. We thank the ODP programme for providing the ODP 977 samples and the R/V *Marion Dufresne* and IMAGES programme for core MD95-2043. We also gratefully thank A. Mackensen, E.J. Rohling and an anonymous reviewer for their helpful comments to this manuscript.

Appendix A

Taxonomic list of the species used in the text. Taxonomic features are those of Hemleben et al. (1989) for extant species.

Neogloboquadrina pachyderma (Ehrenberg, 1861)
Turborotalita quinqueloba (Natland, 1938)
Globorotalia scitula (Brady, 1822)
Globorotalia inflata (d'Orbigny, 1839)
Globigerina bulloides (d'Orbigny, 1826)
Globigerinoides ruber (d'Orbigny, 1839)
Globigerinita glutinata (Egger, 1895)

References

Alley, R.B., Mayewski, P.A., Sowers, T., Stuiver, M., Taylor, K.C., Clarck, P.U., 1997. Holocene climate instability: A prominent, widespread 8200 yr ago. Geology 25, 483–486.

Bé, A.W.H., 1977. An ecological, zoogeographic and taxonomic review of recent planktonic foraminifera. In: Ramsay, A.T.S., (Ed.) Oceanic Micropaleontology, Vol. 1. Academic Press, London, pp. 1–100.

Bé, A.W.H., Tolderlund D.S., 1971. Distribution and ecology of living planktonic foraminifera in surface waters of the Atlantic and Indian Oceans. In: Funnel, B.M., Riedel, W.R. (Eds.), The Micropaleontology of Oceans. Cambridge University Press, London, pp. 105–149.

Bethoux, J.P., 1979. Budgets of the Mediterranean Sea. Their dependence on the local climate and on the characteristics of the Atlantic waters. Oceanol. Acta 2, 157–163.

Bond, G., Heinrich, H., Broecker, W., Labeyrie, L., McManus, J., Andrews, J., Huon, S., Jantschik, R., Clasen, S., Simet, C., Tedesco, K., Klas, M., Bonani, G., Ivy, S., 1992. Evidences for massive discharges of icebergs into the North Atlantic ocean during the last glacial period. Nature 360, 245–249.

Bond, G., Broecker, W., Johsen, S., McManus, J., Labeyrie, L., Jouzel, J., Bonani, G., 1993. Correlations between climate records from North Atlantic sediments and Greenland ice. Nature 365, 143–147.

Bryden, H.L., Kinder, T.H., 1991. Steady two-layer exchange through the Strait of Gibraltar. Deep-Sea Res. 38, S445–S463.

Cacho, I., Grimalt, J.O., Pelejero, C., Canals, M., Sierro, F.J., Flores, J.A., Shackleton, N., 1999. Dansgaard–Oeschger and Heinrich event imprints in Alboran Sea paleotemperatures. Paleoceanography 14, 698–705.

Cacho, I., Grimalt, J.O., Canals, M., Sbaffi, L., Shackleton, N.J., Schönfeld, J., Zahn, R., 2001. Variability of the western Mediterranean Sea surface temperature during the last 25,000 years and its connection with the Northern Hemisphere climatic changes. Paleoceanography 16, 40–52.

Capotondi, L., Borsetti, A.M., Morigi, C., 1999. Foraminiferal ecozones, a high resolution proxy for the Late Quaternary biochronology in the Central Mediterranean Sea. Mar. Geol. 153, 253–274.

Cayre, O., Lancelot, Y., Vincent, E., Hall, M.A., 1999. Paleoceanographic reconstructions from planktic foraminifera off the Iberian Margin: temperature, salinity, and Heinrich Events. Paleoceanography 14, 384–396.

Chapman, M.R., Shackleton, N.J., 1998. Millennial-scale fluctuations in North Atlantic heat flux during the last 150,000 years. Earth Planet. Sci. Lett. 159, 57–70.

Colmenero, E., 2001. Paleoceanografía y estratigrafía de alta resolución en el Golfo de Cádiz en los últimos 40.000 años mediante el estudio de cocolitofóridos. Tesis de Licenciatura, Univ. of Salamanca.

Dansgaard, W., Johnsen, S.J., Clausen, H.B., Dahl-Jensen, D., Gunderstrup, N.S., Hammer, C.V., Hvidberg, C.S., Steffensen, J.P., Sveinbjornsdottin, A.E., Jouzel, J., Bard, G., 1993. Evidence for general instability of past climate from a 250 kyr ice-core record. Nature 364, 218–220.

Dieckmann, G.S., Spindler, M., Lange, M.A., Ackley, S.F., Eicken, H., 1991. Antarctic sea ice: a habitat for the foraminifer *Neogloboquadrina pachyderma*. J. Foraminif. Res. 21, 182–189.

Fairbanks, R.G., Wiebe, P.H., 1980. Foraminifera and Chlorophyll Maximum: vertical distribution, seasonal succession, and paleoceanographic significance. Science 209, 1524–1526.

Fairbanks, R.G., 1989. 17,000-year glacio–eustatic sea level record: influence of glacial melting rates on the Younger Dryas event and deep-ocean circulation. Nature 342, 637–642.

García-Gorriz, E., Carr, M.E., 2001. Physical control of phytoplankton distributions in the Alboran Sea: A numerical and satellite approach. J. Geophys. Res. C 106, 16795–16805.

Grootes, P.M., Stuiver, M., White, J.W.C., Johnsen, S., Jouzel, J., 1993. Comparison of oxygen isotope records from the GISP2 and GRIP Greenland ice cores. Nature 366, 552–554.

Grousset, F.E., Labeyrie, L., Sinko, J.A., Cremer, M., Bond, G., Duprat, J., Cortijo, E., Huon, S., 1993. Patterns of ice-rafted detritus in the Glacial North Atlantic (40–55°N). Paleoceanography 8, 175–192.

Hayes, A., Rohling, E.J., De Rijk, S., Kroon, D., Zachariasse, W.J., 1999. Mediterranean planktic foraminiferal faunas during the last glacial cycle. Mar. Geol. 153, 239–252.

Heburn, G.W., La Violette, P.E., 1990. Variations in the structure of the Anticyclonic Gyres found in the Alboran Sea. J. Geophys. Res. C 95, 1599–1613.

Heinrich, H., 1988. Origin and consequences of cyclic ice rafting in the Northeast Atlantic Ocean during the past 130,000 years. Quat. Res. 29, 142–152.

Hemleben, C., Spindler, M., Anderson, O.R., 1989. Modern Planktic Foraminifera. New York.

Hutson, W.H., 1980. The Agulhas Current during the Late Pleistocene: Analysis of modern faunal analogs. Science 207, 64–66.

Johannessen, T., Jansen, E., Flatoy, A., Ravelo, A.C., 1994.

The relationship between surface water masses, oceanographic fronts and paleoclimatic proxies in surface sediments of the Greenland Iceland and Norwegian seas. In: Zahn, R., Pedersen, T.F., Kaminski M.A., Labeyrie, L. (Eds.), Carbon Cycling in the Glacial Ocean: Constraints on the Ocean's Role in Global Change. NATO Asi Series, I 17, Springer, New York, pp. 61–85.

Jorissen, F.J., Asioli, A., Borsetti, A.M., Capotondi, L., de Visser, J.P., Hilgen, F.J., Rohling, E.J., van der Borg, K., Vergnaud-Grazzini, C., Zachariasse, W.J., 1993. Late Quaternary central Mediterranean biochronology. Mar. Micropaleontol. 21, 169–189.

Kallel, N., Paterne, M., Duplessy, J.C., Vergnaud-Grazzini, C., Pujol, C., Labeyrie, L., Arnold, M., Fontugne, M., Pierre, C., 1997. Enhanced rainfall in the Mediterranean region during the last sapropel event. Oceanol. Acta 20, 697–712.

Kudrass, H.R., 1973. Sedimentation am Kontinentalhang vor Portugal und Marokko im Spätpleistozän und Holozän. Meteor Forschungsergeb. C 13, 1–63.

Kudrass, H.R., Thiede, J., 1970. Stratigraphische Untersuchungen an Sedimentkernen des ibero–marokkanischen Kontinentalrandes. Geol. Rundsch. 60, 294–391.

Lebreiro, S.M., Moreno, J.C., McCave, I.N., Weaver, P.P.E., 1996. Evidence for Heinrich layers off Portugal (Tore Seamount: 39°N, 12°W). Mar. Geol. 131, 47–56.

Levitus, S., 1982. Climatological Atlas of the World Ocean. NOAA Prof. Pap., US Govt. Print. Office, Washington, DC.

Manighetti, B., McCave, I.N., Maslin, M., Shackleton, N.J., 1995. Chronology for climate change: developing age models for the biogeochemical ocean flux study cores. Paleoceanography 10, 513–525.

Martinson, D.G., Pisias, N.G., Hays, J.D., Imbrie, J., Moore, T.C., Shackleton, N.J., 1987. Age dating and the orbital theory of the ice ages: development of a high-resolution 0 to 300,000-year chronoestratigraphy. Quat. Res. 27, 1–29.

Overpeck, J.T., Webb, T., III, Prentice, I.C., 1985. Quantitative interpretation of fossil pollen spectra: dissimilarity coefficients and the method of Modern Analog. Quat. Res. 23, 87–108.

Parrilla, G., 1984. Preliminary results of the ¿Donde Va? experiment. Informe Técnico 24, Inst. Esp. Oceanogr., Madrid.

Parrilla, G., Kinder, T.H., 1987. Oceanografía física del Mar de Alboran. Bol. Inst. Esp. Oceanogr. 4, 133–165.

Paterne, M., Kallel, N., Labeyrie, L.D., Vautravers, M., Duplessy, J.C., Rossignol-Strick, M., Cortijo, E., Arnold, M., Fontugne, M., 1999. Hydrological relationship between the North Atlantic Ocean and the Mediterranean Sea during the past 15–75 kyr. Paleoceanography 14, 626–638.

Prell, W.L., 1985. The stability of low-latitude sea-surface temperatures: An evaluation of the CLIMAP reconstruction with emphasis on the positive SST anomalies. US Department of Energy, Technical Report (TRO25), Brown University.

Pujol, C., Vergnaud-Grazzini, C., 1989. Paleoceanography of the Last Deglaciation in the Alboran Sea (Western Mediterranean). Stable isotopes and planktic foraminiferal records. Mar. Micropaleontol. 15, 153–179.

Pujol, C., Vergnaud-Grazzini, C., 1995. Distribution patterns of live planktic foraminifers as related to regional hydrography and productive systems of the Mediterranean Sea. Mar. Micropaleontol. 25, 187–217.

Reguera, I., 2001. Paleoceanografía y estratigrafía de alta resolución en el Golfo de Cádiz en los últimos 40.000 años mediante el estudio de foraminíferos planctónicos. Tesis de Licenciatura. Univ. of Salamanca.

Reynolds, L.A., Thunell, R.C., 1986. Seasonal production and morphologic variation of *Neogloboquadrina pachyderma* (Ehrenberg) in the northeast Pacific. Micropaleontology 32, 1–18.

Rodríguez, J., Blanco, J.M., Jiménez-Gómez, F., Echevarría, F., Gil, J., Rodríguez, V., Ruiz, J., Bautista, B., Guerrero, F., 1998. Patterns in the size structure of the phytoplankton community in the deep fluorescence maximum of the Alboran Sea (southwestern Mediterranean). Deep-Sea Res. I 45, 1577–1593.

Rohling, E.J., Bryden, H.L., 1994. A method for estimating past changes in the eastern Mediterranean freshwater budget, using reconstructions of sea level and hydrography. Proc. K. Ned. Akad. Wet. B 97, 201–217.

Rohling, E.J., Hayes, A., De Rijk, S., Kroon, D., Zachariasse, W.J., Eisma, D., 1998. Abrupt cold spells in the Northwest Mediterranean. Paleoceanography 13, 316–322.

Rohling, E.J., Den Dalk, M., Pujol, C., Vergnaud-Grazzini, C., 1995. Abrupt hydrographic change in the Alboran sea (Western Mediterranean) around 8000 yrs BP. Deep-Sea Res. 42, 1609–1619.

Sbaffi, L., Wezel, F.C., Kallel, N., Paterne, M., Cacho, I., Ziveri, P., Shackleton, N., 2001. Response of the pelagic environment to paleoclimatic changes in the central Mediterranean Sea during the Late Quaternary. Mar. Geol. 178, 39–62.

Stuiver, M., Reimer, P.J., Bard, E., Beck, W., Burr, G.S., Hughen, K.A., Kromer, B., McCormac, F.G., van der Plicht, J., Spurk, M., 1998. INTCAL98 radiocarbon age calibration, 24,000 cal BP. Radiocarbon 40, 1041–1083.

Tintoré, J., LaViolette, P., Blade, I., Cruzado, A., 1988. A study of an intense density front in the Eastern Alboran Sea: the Almería–Orán front. J. Phys. Oceanogr. 18, 1384–1397.

van Kreveld, S.A., Knappertsbusch, M., Ottens, J., Gaussen, G.M., van Hinte, J.E., 1996. Biogenic carbonate and ice-rafted debris (Heinrich layer) accumulation in deep-sea sediments from a Northeast Atlantic piston core. Mar. Geol. 131, 21–46.

Volkman, J.K., Eglinton, G., Corner, E.D.S., Forsberg, T.E.V., 1980. Long-chain alkenes and alkenones in the marine coccolitophorid *Emiliania huxleyi*. Phytochemistry 19, 2619–2622.

Zahn, R., Schönfeld, J., Kudrass, H.R., Park, M.H., Erlenkeusser, H., Grootes, P., 1997. Thermohaline instability in the North Atlantic during meltwater events: Stable isotope and ice-rafted detritus records from core SO75-26KL, Portuguese margin. Paleoceanography 12, 696–710.